JOURNAL OF NANO- AND ELECTRONIC PHYSICS
Vol. **10** No 5, 05008(5pp) (2018)

ЖУРНАЛ НАНО- ТА ЕЛЕКТРОННОЇ ФІЗИКИ
Том **10** № 5, 05008(5cc) (2018)

A Perspective on Zinc Oxide Based Diluted Magnetic Semiconductors

Rana Mukherji[1,*], Vishal Mathur[1,†], M. Mukherji[2,‡]

[1] *The ICFAI University, Jaipur, India*
[2] *Amity University Rajasthan, Jaipur, India*

(Received 25 July 2018; revised manuscript received 20 October 2018; published online 29 October 2018)

Diluted magnetic semiconductor (DMS) is envisaged to portray a substantial position in inter-punitive material science and prospect spintronics. The reason being spin and charge degrees of freedom are accommodated into solitary matter and their interaction is anticipated to probe innovative electronic devices. DMSs evince multifarious advantages such as wide band gap apposite for applications with short wavelength light, transparency and dye ability with pigments, high carrier concentration, capability to be cultivated even on plastic substrate at low temperature, green safety, durability , most importantly economical. Various theoretical and experimental research findings have been proposed on the ferromagnetic, paramagnetic, antiferromagnetic and spin glass properties at room-temperature of transition metal-doped DMSs such as TiO_2, ZnO, Cu_2O, SnO_2, In_2O_3 etc in last few years. The objective of the paper is to comprehend the recent research advancement of ZnO based DMS specimens doped with various 3d transition metals.

Keywords: Spintronics, Dilute magnetic semiconductors (DMS), Room temperature, Ferromagnetism (RTFM), Zinc oxide (ZnO).

DOI: 10.21272/jnep.10(5).05008 PACS numbers: 85.75.d, 75.50.Pp, 75.50.Bb, 77.84.Bw

1. INTRODUCTION

Moore's law foresees a biennial two-fold increase in the number of transistors in a single chip. Though, the potentiality to keep deflating transistor size and squashing ever further onto silicon chips is attaining its physical limit [1]. Hence, alternative methodologies to orthodox electronics are to be explored which are fundamentally diverse and need different computational proficiencies. Spintronics (shorthand for "spin electronics"), has appeared to be a stout alternative emergent technology to this. Basically, it is a technology that works by maneuvering the spin of electrons, instead of depending only on their charge. Spintronic devices can offer higher computing speeds and storage capacities, at lower power consumption, than traditional silicon chips [2]. Diluted magnetic semiconductors (DMS) are the material of technological attention as they own the potentiality for the future era of spintronics devices. The DMS evinces multifarious advantages such as wide band gap apposite for applications with short wavelength light, transparency and dye ability with pigments, high carrier concentration, capability to be cultivated even on plastic substrate at low temperature, green safety, durability, most importantly economical [3]. Various theoretical and experimental research findings have been proposed on the ferromagnetic, paramagnetic, antiferromagnetic and spin glass properties of transition metal (TM)-doped DMSs such as TiO2, ZnO, Cu2O, SnO2 as well as In2O3 [4]. Among these, ZnO is one of most predominant affiliate of DMS cluster comprising band gap of ~ 3.37 eV, resistivity (~ 10-2 cm) and excessive excitation binding energy (~ 60 meV) [5]. It displays a wurtzite structure (P63 mc) with lattice parameters $a = 3.2539$ A and $c = 5.2098$ A°. It is noticed that with a certain appropriate doping into ZnO, an exceedingly conductive (3.7×10^{-3} cm) specimen with decent optical transparency (~ 80 – 85 %) and extraordinary carrier density (1.7×1020 cm^{-3}) can be synthesized [6]. In the previous couple of decades, researchers had explored the impact of doping ZnO nanoparticles with TMs, for eg., Ni,Co, Fe, and Mn by utilizing the deformity interrelated mechanism, bound magnetic polarons (BMPs), hole mediated exchange interaction, ancillary phase and concocting system at lower and higher Curie temperature. There are several reports available in the literature on optical and electrical properties of transition metal doped ZnO, but still it is a decent candidate for obtaining room temperature ferromagnetic properties, which are of significant prominence in low dimensional memory devices [7]. The paper deals with perspective of the developments in the area of synthesis and characterization of ZnO based dilute magnetic semiconductors.

2. CRYSTAL STRUCTURES

Zinc oxide materializes in hexagonal wurtzite, cubic zinc blende, also, rarely apparent cubic rocksalt (see Fig. 1 (a)-(c)). The wurtzite structure is eminently stable and rampant at atmospheric conditions. The zinc blende configuration is made stable by developing ZnO on substrates with cubic lattice structure. It is noticeable that the ZnO is tetrahedral in both the configurations. The rocksalt NaCl-type structure is solitarily perceived at pressure ~ 10 GPa.

The zinc blende and hexagonal ZnO lattices do not have transposal symmetry, which means, the mirror

* rana.mukherji@gmail.com
† wishalmathur@gmail.com
‡ manishita@outlook.com

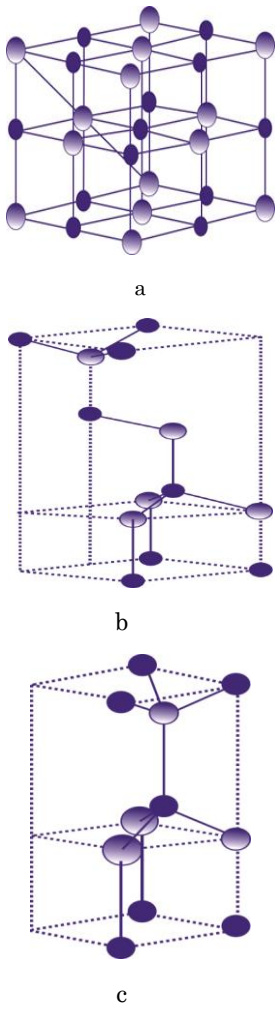

Fig. 1 – ZnO structures: (a) cubic rocksalt, (b) cubic zinc blende, and (c) hexagonal wurtzite [7]

image of the crystal relatively at any given point does not transmute it into itself. This and new lattice symmetry properties leads to pyro-electricity of hexagonal ZnO and in piezoelectricity of the both hexagonal and zinc blende ZnO.

The hexagonal structure own a point group 6 mm *(Hermann-Mauguin notation)* or C6v *(Schoenflies notation)* and belong to space group P63mc. The lattice constants are $a = 3.25$ Å and $c = 5.2$ Å; their ratio c/a is about 1.60 which is proximate to the standard value for hexagonal cell i.e. $c/a = 1.633$. ZnO is fundamentally ionic utmost II-VI material, which elucidates its strong piezoelectricity. Consequently, zinc and oxygen planes exhibit electric charges (positive and negative, respectively) [8].

Thus, to sustain electrical neutrality, those planes are reconstructed at atomic level in utmost relative materials, nevertheless, not in ZnO as its surfaces are atomically smooth, stable and evince no reconstruction. This aberration of ZnO is not abundantly studied yet.

3. ELECTRONIC PROPERTIES

ZnO has a comparatively substantial direct band gap of ~ 3.3 eV; thus, pristine ZnO is achromic and transpicuous. The benefits of large band gap comprise of greater breakdown voltages, capability to bear substantial electric fields, lesser noise, additionally suitability of elevated temperature as well as power operations. Moreover, the bandgap of ZnO can be tweaked from ~ 3-4 eV by amalgamating with magnesium oxide or cadmium oxide [9].

Mainly, ZnO has *n*-type character, even with the lack of intense doping. Innate defects, as an example, oxygen vacancies or zinc interstitials are frequently anticipated to be the source of the same, despite that the study stays contentious. A substitute explication has been proffered based on theoretical calculations which statesabout the accountability of unintended bartering of hydrogen impurities [10]. Controllable n-type doping is comfortably consummated either by replacing Zn atoms with 3*d* group elements like Al, Ga, In or by replacing oxygen with group-VII elements like Cl or I. Definitive *p*-type doping of ZnO remnants are still challenging. This quandary emanates from low solubility of p-type dopants and their atonement by plentiful n-type impurities which are not apt solely to ZnO. Hence, measurement of p-type in "intrinsically" *n*-type material is arduous. The absenteeism of *p*-type ZnO constrains its electronic and optoelectronic applications which generally necessitate junctions of n and p-type material. Known p-type dopants embrace group-I elements like Na, Li, K; group-V elements As, P and N; as well as Ag and Cu. Though, numerous p-type dopants form deep acceptors, also, do not yield noteworthy p-type conduction at room temperature. Electron mobility of ZnO strappingly diverges with temperature and has a maxima of ~ 2000 $cm^2/(V\,s)$ at approximately 80 K. Data on hole mobility are rare with values in the array around 530 $cm^2/(V\,s)$ [11].

ZnO is an alluring material for applications in electronics, photonics, acoustics and sensing. Accordingly, it has solid potential to be a prominent contender for upcoming era of spintronic gadgets. In this segment, recent progresses in electrical, optical and magnetic properties with basic issues for realization of ZnO-based DMSs have been discussed.

4. IMPACT OF VARIOUS TMS DOPING IN ZnO

Early reviews on DMS materials started with Mn-doped II-VI composites of the form AII $BVI_{1-x}Mn_x$ (where AII = Zn, Cd, Hg and BVI = S, Se, Te) in 1980s [12]. Mao et al [13] synthesized Zinc oxide (ZnO) nanofibers doped with Mn by electro spinning followed by calcinations at 580 °C for 2.5 hours. They revealed that the diameters of $Zn_{1-x}Mn_xO_3$ nanofibers are between 60-90 nm corresponding to the Mn concentration between 0-2 wt %. They also confirmed that Mn^{2+} ions are present in + 2 state. Mote et al [14] synthesized $Zn_{1-x}Mn_xO_3$ by sol–gel route and sintered at 400 °C. They found that the dielectric constant and dielectric loss declines with inclination of Mn concentration and frequency. De Almeida et al [15] explained about RTFM behaviour association with PM Curie–Weiss component. The density and magnetization of defects dramatically diminishes after the post-sintering.

Ni doped ZnO is another prime competitor from the view purpose of straightforwardness and attraction for

potential *Optical Incorporated Circuit* (OIC) and optical application in short wavelength field [16]. From the research perspective, the magnetic properties of the $Zn_{1-x}Ni_xO_3$ are not caught on. Snure et al [17] found that ZnO:Ni films placed under 10^{-6} Torr of pressure shows hysteresis at room temperature. Amid all the known $Zn_{1-x}TM_xO_3$ systems, Ni-based materials are likely the utmost disputable. There is a lot of contention and discussion over the beginning of FM in these materials and the stated assortment in magnetic moments. Liu et al [18] showed that FM of the Ni-doped ZnO nanoparticles originated from the presence of the V_o (*oxygen vacancy*). They also depicted that the saturated magnetization firstly increases and then decreases with increase of Ni concentration, which results from the competition between oxygen vacancies and antiferromagnetic coupling between Ni^{2+} in NiO. Pal et al [19] reported the RTFM in the $Zn_{1-x}Ni_xO$ ($x = 0$, 0.03 and 0.05) amalgamated by a ball milling route. They highlighted the influence of changing defect density on the observed FM moment values. They also revealed that both the natures of Ni^{2+} ions as well as the defects are noteworthy constituents responsible for achieving high moment as well as high ordering temperature in $Zn_{1-x}Ni_xO$ specimens.

Cr doping is also energetically favourable doping element to achieve room temperature ferromagnetism. Singh et al [20] studied the structural and optical properties of $Zn_{1-x}Cr_xO$. They evinced the films were highly transparent (~ 90 %) in the visible region, which reduces with chromium doping. The band gap initially increases for low Cr-concentration and then decreases with higher Cr-concentration. Kumar et al [21] also studied optical properties and concluded that singly ionized oxygen vacancies, increases with an increase in Cr doping concentration in the specimens.

Gürbüz et al [22] observed a reduction of grain size with an inclination of Cr content in ZnO resulting, reduction in the dielectric constants whereas an inclination in loss tangents. Moreover, a reduction in electrical resistivity of specimens observed amid 29.8 – 0.403 mΩ cm with the upsurge in Cr content.

Wojnarowicz et al [23] blended ZnO-Co by the typical microwave solvo-thermal synthesis route. They investigated a relationship between local structures, valence of the Co atoms and that in turn the valency stoutly clouts the prominent carrier type with magnetism in the Zn-Co-O system. Fabbiyola et al [24] mixed ZnO and Co^{2+} by coprecipitation technique in which specimens were dried at 200 °C for 1 h followed by sintering at 500 °C for 3 h. They observed that the crystallites size and band gap of pure ZnO decreases as Co^{2+}dopant concentration increases. Pazhanivelu et al [25] successfully synthesized Co doped ZnO nanoparticles by the co-precipitation technique. The XRD assessment affirms that the wurtizite structure for the $Zn_{1-x}Co_xO$ nano-particles was successfully synthesized. Furthermore, the peaks shift was noticeable with the upsurge of Co contents in ZnO matrix. The cell volume, average crystallite size, lattice parameters and bond length were reduced with the intensification of dopant content, the reason being lesser ionic radius of the Co ions amalgamation in the ZnO lattice. The determined RTFM within the ready specimens could be initiating from Co ion insertion in ZnO matrix additionally owing to the oxygen vacancies.

El Ghoul et al [26] also synthesized $Zn_{1-x}Co_xO$ ($0 \le x \le 0.05$) nanoparticles by sol-gel route and observed a diamagnetic behaviour for undoped ZnO and $Zn_{1-x}Co_xO$ ($x = 0.01$), but with the upsurge in doping concentration ($x = 0.03$ and 0.05), magnetization plots indicated that the specimen has both PM and FM behaviour respectively.

Mahmood et al [27] studied the first principles based on density functional theory. In their findings, $Zn_{0.75}Co_{0.25}Te$ exhibited feeble ductile behavior but large magnetic moment is observed at the magnetic atomic sites. However, small magnetic moments at non-magnetic sites (Zn and Te) are also found due to hybridization of *p*- and *d*-states.

Mukherji [28] blended polycrystalline specimen of ($Zn_{1-x}Co_xO$; $x = 0.06$) by the typical solid state reaction route. The blended specimens are then hydrogenised for ~ 10 hours at 550 °C in a cylindrical quartz tube in a reduction furnace. Afterwards, hydrogenated specimens were further heated for 2 and 7 hours in air respectively. They evinces that Co^{2+} ions replace the

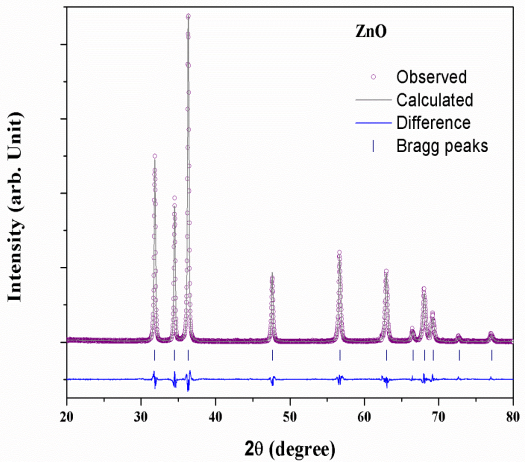

a

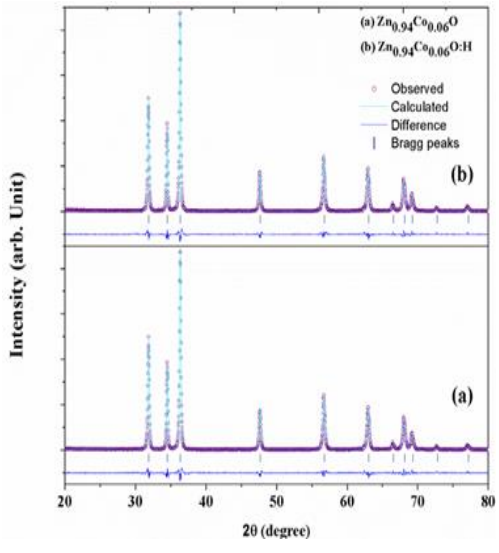

b

Fig. 2 – Refined XRD scans of (a) ZnO, (b) $Zn_{0.94}Co_{0.06}O_3$ and $Zn_{0.94}Co_{0.06}O_3$:H

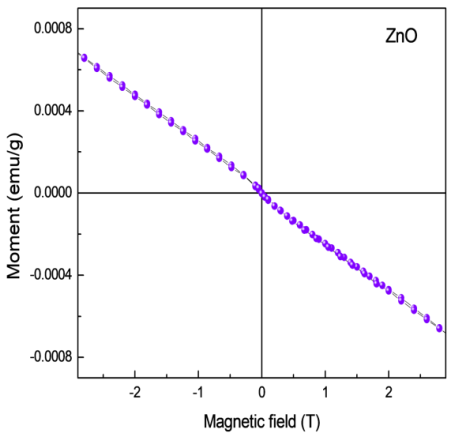

Fig. 3 – M-H curve for pure ZnO measured at 300 K

Zn^{2+} site and no structural change has been noted even after the annealing in hydrogen atmosphere through the X-ray diffractograms (see Fig. 2(a)-(b)).

The M-H plot findings reveals that ZnO ($x = 0.00$) exhibit a diamagnetic demeanour at 300 K as a negation in susceptibility (see Fig. 3). The M-H plots for the Co doped ZnO specimens are as shown in Fig. 4 (a)-(c) and Fig. 5 (a)-(d). It is observed that Co doping turns the diamagnetic properties of ZnO into paramagnetic. Experimental findings also depict that on hydrogenation, the specimens achieved significant ferromagnetic properties overwhelming the diamagnetic properties of ZnO, confirming the act of hydrogen in ZnO as a shallow donor impurity which delivers deliver additional free electrons. This study also depicts that all the specimens of hydrogenated Co doped ZnO finally resumed (after 7hours air sintering) to the paramagnetic state.

Cernea et al [29] synthesized polycrystalline $Zn_{1-x}Fe_xO$ ($x = 0$, 0.01 and 0.03) by hydrothermal technique at 200 °C, 2h. The grains of specimen altered their shape from floret-like shape to hexagonal prisms as Fe concentration (x) increases. They found that both undoped and Fe doped ZnO revealed RTFM and magnetization upsurges with enhancement in Fe contents which indicated that Fe^{3+} ions participate at FM in doped ZnO. Singh et al [30] studied the impact of calcination on the magnetic properties of $Zn_{1-x}Fe_xO$ specimens. Their findings revealed that coercivity and remanent polarization increase with increase in

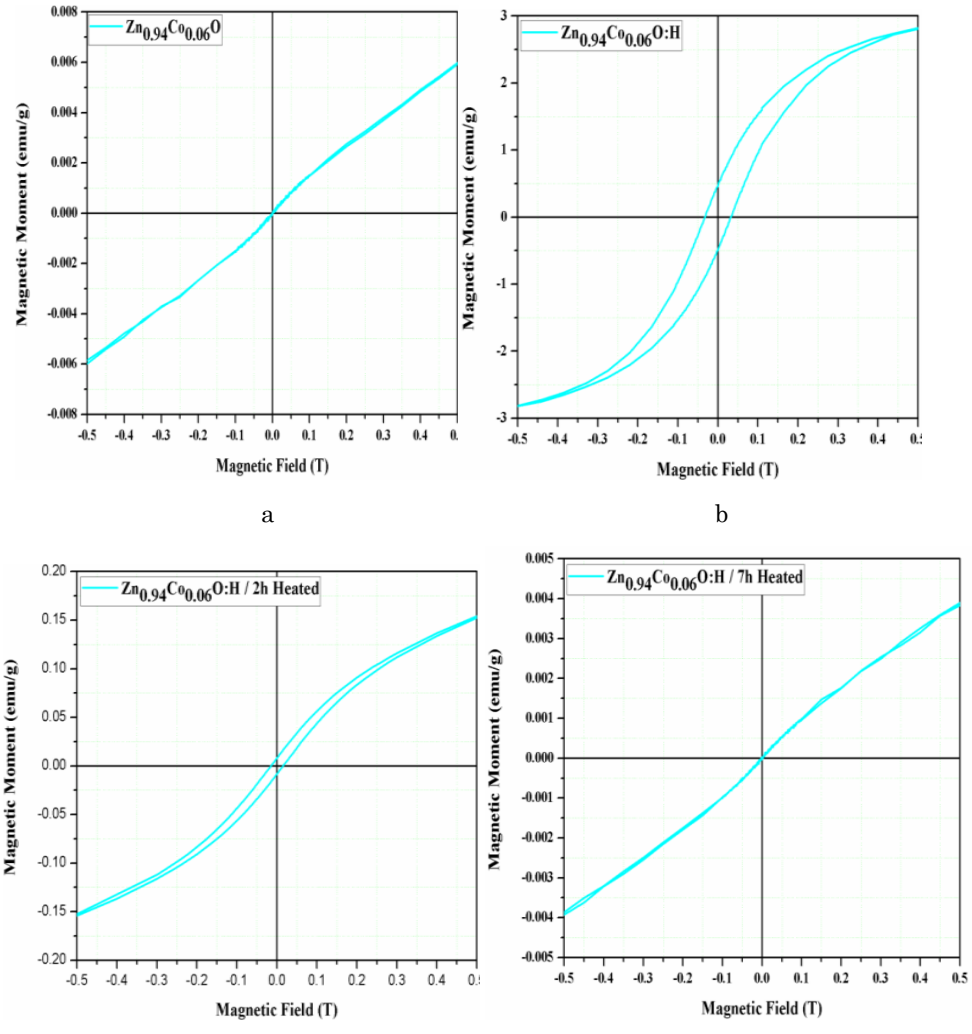

Fig. 4 – M-H curves recorded at 300 K for (a) $Zn_{0.94}Co_{0.06}O_3$, (b) $Zn_{0.94}Co_{0.06}O_3$:H (c) $Zn_{0.94}Co_{0.06}O_3$:H (2 hours heated) and (d) $Zn_{0.94}Co_{0.06}O_3$:H (7 hours heated)

calcination temperature from 450 °C to 750 °C; whereas, reverse effect was observed for magnetization saturation.

Kafle et al [31] investigated the crystallinity, surface morphology and optical properties of $Zn_{1-x}Fe_xO$ films. They prepared specimens using spin coating technique and observed that when Fe ions contents were steadily increased, the haphazardly oriented matrix shaped nanoparticles altered to cylindrical long grains.

Kumar et al [32] used chemical co-precipitation method to blende $Zn_{1-x}Fe_xO$ particles with distinct concentration. They found that specific magnetization photocatalytical, optical and magnetic properties of $Zn_{1-x}Fe_xO$ depend on dopant concentration.

Raja et al [33] did an exploration on $Zn_{1-x}Fe_xO$ ($x = 0$, 0.03, 0.06 and 0.09) nanopowder which was prepared by co-precipitation method sintered at 550 ˚C. They found that the hydrogenated specimens have improved crystalline structure and optical properties. Straumal et al [83] explained the impact of the grain boundary specific area on the appearance of ferromagnetism in Fe-doped ZnO.

5. CONCLUSION

The paper affirmed about the RTFM in ZnO based dilute magnetic semiconductors. The dissimilitude of outcomes discussed in the article evidently reveals the snag in understanding the cause of RTFM in these DMSs. Few group of the scientific communal found RTFM owing to the substitution of doped TM into the ZnO while others achieved RTFM after annealing in vacuum/H_2/air or any other medium.

REFERENCES

1. G.E. Moore, *Electronics* **38**, 114 (1965).
2. C.H. Marrows, B.J. Hickey, *Philos. Trans. Roy. Soc A* **369**, 3027 (2011).
3. A.A. Dakhel, *J. Super. Cond. Nov. Magn.* **28**, 2039 (2015).
4. N. Aggarwal, A. Vasishth, B. Singh, *Integr. Ferroelectr.* **186**, 10 (2018).
5. S. Zaineb, S. Atiq, A. Mahmood, S.M. Ramay, S. Riaz, and S. Naseem, *J. Mater. Sci. Mater. El.* **29**, 3943 (2018).
6. S. Nagar, S. Chakrabarti, *Introduction: In Optimization of ZnO Thin Films* (Springer Singapore: 2017).
7. G. Srinet, *PhD Thesis* (Jaypee Institute of Information Technology, India: 2015).
8. D.C. Look, *Mater Sci. Eng. B* **80**, 383 (2001).
9. Y.Q. Fu, J.K. Luo, X.Y. Du, A.J. Flewitt, Y. Li, G.H. Markx, A.J. Walton, W.I. Milne, *Sensor. Actuat. B-Chem.* **143**, 606 (2010).
10. Ö. Ümit, D. Hofstetter, H. Morkoc, *Proc. IEEE* **98**, 1255 (2010).
11. C. Liu, F. Yun, H. Morkoc, *J. Mater. Sci. Mater. El.* **16**, 555 (2005).
12. N.A. Theodoropoulou, A.F. Hebard, D.P. Norton, J.D. Budai, L.A. Boatner, J.S. Lee, Z.G. Khim, Y.D. Park, M.E. Overberg, S.J. Pearton, R.G. Wilson. *Solid State Electron* **47**, 2231(2003).
13. Y. Mao, S. Ma, X. Li, C. Wang, F. Li, X. Yang, J. Zhu, L. Ma, *Appl. Surf. Sci.* **298**, 109 (2014).
14. V.D. Mote, Y. Purushotham, B.N. Dole, *Mater. Design.* **96**, 99 (2016).
15. V.M. De Almeida, A. Mesquita, A.O. De Zevallos, N.C. Mamani, P.P. Neves, X. Gratens, V.A. Chitta, W.B. Ferraz, A.C. Doriguetto, A.C.S. Sabioni, H.B. De Carvalho, *J. Alloy. Compd.* **655**, 406 (2016).
16. X. Mao, W. Zhong, Y. Du, *J. Magn. Magn. Mater.* **320**, 1102 (2008).
17. M. Snure, D. Kumar, A. Tiwari, *Appl. Phys. Lett.* **94**, 012510 (2009).
18. Y. Liu, H. Liu, Z. Chen, N. Kadasala, C. Mao, Y. Wang, Y. Zhang, H. Liu, Y. Liu, J. Yang, Y. Yan, *J. Alloy. Compd.* **604**, 281 (2014).
19. B. Pal, D. Sarkar, P.K. Giri, *Appl. Surf. Sci.* **356**, 804 (2015).
20. D. Singh, K. Rawat, P. Pal, P.K. Shishodia, *Emerg. Mater. Res.* **5**, 182 (2016).
21. S. Kumar, N. Tiwari, S.N. Jha, S. Chatterjee, D. Bhattacharyya, A.K. Ghosh, *RSC Adv.* **6**, 107816 (2016).
22. O. Gürbüz, M. Okutan, *Appl. Surf. Sci.* **387**, 1211 (2016).
23. J. Wojnarowicz, S. Kusnieruk, T. Chudoba, S. Gierlotka, W. Lojkowski, W. Knoff, T. Story, Beilstein, *J. Nanotech.* **6**, 1957 (2015).
24. S. Fabbiyola, L.J. Kennedy, U. Aruldoss, M. Bououdina, A.A. Dakhel, *J. Judith. Vijaya. Powder Tech.* **286**, 757 (2015).
25. V. Pazhanivelu, A.P.B. Selvadurai, R. Murugaraj, I.P. Muthuselvam, F.C. Chou, *J. Mater. Sci. Mater. El.* **27**, 8580 (2016).
26. J. El Ghoul, M. Kraini, O.M. Lemine, L. El Mir, *J. Mater. Sci. Mater. El.* **26**, 2614 (2015).
27. Q. Mahmood, A. Javed, G. Murtaza, S.M. Alay-e-Abbas, *Mater. Chem. Phys.* **162**, 831 (2015).
28. R. Mukherji, *PhD Thesis. The ICFAI University*, Jaipur, India (2017).
29. M. Cernea, V. Mihalache, E.C. Secu, R. Trusca, V. Bercu, L. Diamandescu, *Superlatt. Microst.* **104**, 362 (2017).
30. P. Singh, R. Preet, I.S. Hudiara, S. Bhushan Rana. *Mater. Sci. Poland.* **34**, 451 (2016).
31. B.P. Kafle, S. Acharya, S. Thapa, S. Poudel, *Ceram. Int.* **42**, 1133 (2016).
32. K. Kumar, M. Chitkara, I.S. Sandhu, D. Mehta, S. Kumar, *J. Alloy. Compd.* **588**, 681 (2014).
33. K. Raja, P.S. Ramesh, D. Geetha, *Spectrochim. Acta. A.* **131**, 183 (2014).